

NEAR-SURFACE LIGHTING ESTIMATION AND RECONSTRUCTION

Qian Zhang^{1,2}, Fei-Peng Tian^{1,2}, Rui-Ze Han^{1,2}, Wei Feng^{1,2}*

¹ School of Computer Science and Technology, Tianjin University, Tianjin, China

² Key Research Center for Surface Monitoring and Analysis of Cultural Relics,

State Administration of Cultural Heritage, China

{qianz,tianfeipeng,han_ruize,wfeng}@tju.edu.cn

ABSTRACT

In this paper, we propose an effective approach to estimating a near-surface lighting function from a limited number of images captured under different illuminations. Unlike classical methods relying on simplified parallel lighting model or near-point lighting model, our approach directly focuses on the much more realistic near-surface light source and formulates it as a regular grid of near-point light sources. We present an iterative joint optimization strategy to solve the scene normal, reflectance and near-point light source positions. Based on such new model, reliable relighting under arbitrary new illuminations can be faithfully reconstructed by applying the given lighting condition to the same scene. Experiments show that the proposed approach can generate more accurate relighting results than state-of-the-art competitors.

Index Terms— Lighting estimation and reconstruction, photometric stereo, near-point lighting model

1. INTRODUCTION

Image reconstruction is a problem that involves simulating a realistic scene image under a given lighting condition. In theory, the reconstructed image has potential for use in many tasks such as exhibition or monitoring of cultural heritage [1, 2, 3]. A related technology is photometric stereo (PS), which aims to acquire the scene normal and reflectance from several images taken from the same camera viewpoint but under different lighting conditions. The existing photometric stereo methods always attempt to solve the inverse problem of a specific physical lighting model. The original photometric stereo methods [4, 5] assume that the scene of interest is a Lambertian surface and all the scene points have the same lighting incidence direction that needs to be calibrated. These methods have shown good results but still leave room for further research. First, the lighting incidence direction assumption is a reasonable approximation if the lighting

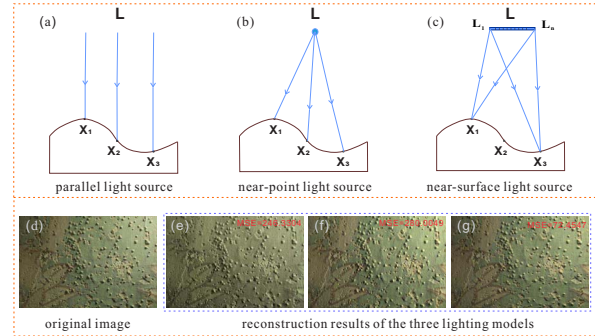


Fig. 1. The three lighting models and their reconstruction results. (a) The parallel lighting condition. (b) The near-point condition. (c) The near-surface lighting condition. (d) Original image. (e)-(g) The reconstruction results of the three lighting models, respectively.

is infinitely far from the scene, but capturing images with distant lighting is unrealistic in fact. Second, the scene surface always exists in various textures or structures and may exhibit many specific situations such as specular reflection, shadow and internal reflection. In other words, the simplified lighting model will influence the reconstruction accuracy seriously.

To address the limitations of the traditional model, various types of extensions have been proposed, including the methods that consider lighting-calibration-free [6, 7, 8, 9, 10] or non-Lambertian surface [11, 12, 13, 14, 15, 16, 17]. All of these methods are based on the assumption of distance lighting, i.e., the scene points receive the incident light from the same direction, as shown in Fig. 1(a). However, a light source cannot be located at an infinite point in the real scene and different scene points usually have different incident light directions, as shown in Fig. 1(b). Furthermore, the lighting irradiance falls by the square of distance between light source position and scene point in theory. Many methods with the near-point lighting model have been proposed [18, 19, 20, 21, 22, 3, 23] and the near-point lighting model always addresses a nonlinear problem in general. [3, 23] solve the scene information and lighting conditions alternately through an iterative strategy, [20] explores the linear representation by mesh deformation to the near-

* is the corresponding author. Tel: (+86)-22-27406538. This work is supported by NSFC (61671325, 61572354) and the National Science and Technology Support Project (2014BAK07B03).

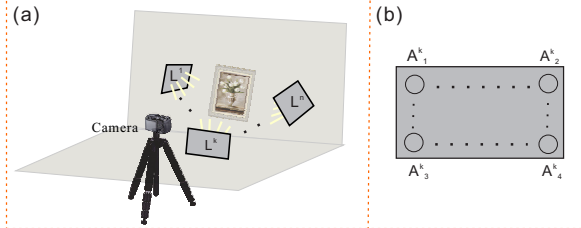


Fig. 2. (a) Near-surface lighting model reflects both the position and orientation. (b) Near-surface light source can be regarded as a combination of several virtual point light sources.

point lighting model, and [18] converts the non-linear problem based on the assumption that the irradiance attenuation is only proportional to the distance. The near-point lighting model is more reasonable than parallel lighting model under realistic lighting condition, and parallel lighting model always tends to generate the potato-chip shape error [3].

In practice, both the parallel lighting model and the near-point lighting model are unreasonable. As shown as Fig. 1(c), a more real condition is surface light source. In this paper, we propose a novel near-surface lighting model. To the best of our knowledge, this study represents the first time that this model has been proposed. Then, we solve the scene normal, reflectance, and lighting positions by using an iterative strategy similar to the method proposed by [3]. Our method is calibration-free and can acquire more accurate reconstruction results than the state-of-the-art with parallel lighting model or near-point lighting model. Fig. 1(d) Fig. 1(g) show the reconstruction results of the three lighting models. Fig. 1(d) presents the original image, and Fig. 1(e) and Fig. 1(f) indicate the reconstruction results reported by [8] and [3], respectively. Fig. 1(g) shows the result of our method. We can observe that our method can acquire higher reconstruction accuracy than other methods.

Our major contribution is three-fold:

1. **A near-surface lighting generalization.** To the best of our knowledge, we first propose the near-surface lighting model, which can be formulated as a regular grid of near-point light sources.
2. **An calibration-free solution.** Our approach is an calibration-free model and does not need any prior knowledge about the light source.
3. **High accuracy of image reconstruction.** We reconstruct the scene image under a given lighting condition and acquire better results than those of the state-of-the-art methods.

2. OUR APPROACH

Notation. In this paper, \mathbf{I} stands for the captured images, \mathbf{R} and \mathbf{N} are scene reflectance and normal, respectively. K and P are the indexes of different images and pixels, i.e., \mathbf{I}_p^k indicate the p th pixel intensity of the k th image, and \mathbf{R}_p and \mathbf{N}_p

denote the corresponding reflectance and normal positions of the p th pixel.

2.1. Problem Formulation

Traditional photometric stereo methods are based on the parallel lighting model or the near-point lighting model. However, perfect parallel lighting and near-point lighting are nonexistent in fact. Thus, we propose a novel near-surface lighting model and we solve the scene normal, reflectance, and lighting positions through an iterative strategy. Then, we recover the scene image under a given lighting condition. In this task, the proposed method generates more accurate reconstruction results than those of the other two lighting models. Our method is calibration-free and the only inputs are multiple images captured from the same camera viewpoint under different lighting conditions.

2.2. Near-surface Lighting Model

First, we discuss the near-point lighting model, which was first proposed by Frolova et al. [24] in 2004. As shown in Fig. 1(b), because of the near lighting assumption, every scene point has a different incident light direction. With an isotropic point light source with power e at position \mathbf{L} , the scene image can be represented approximately by

$$\mathbf{I}_p^k \approx \mathbf{R}_p \cdot \frac{e}{\|\mathbf{L}^k - \mathbf{X}_p\|} \cdot \frac{\mathbf{N}_p^T (\mathbf{L}^k - \mathbf{X}_p)}{\|\mathbf{L}^k - \mathbf{X}_p\|}, \quad (1)$$

where \mathbf{L}^k is light source position of the k th image, and \mathbf{X}_p indicates the spatial coordinate of the p th scene point. $\frac{e}{\|\mathbf{L}^k - \mathbf{X}_p\|^2}$ denotes that the lighting power e falls by the square of distance between light source position and the scene point.

Based on the near-point lighting model, a novel near-surface lighting model was proposed in this paper. As shown in Fig. 2(b), a surface light source can be regarded as a combination of several virtual point light sources and all of them are arranged in a rectangle. We define the row and column numbers of the point lighting matrix as M and N and the coordinates of the point light sources located in the four corners of the rectangle as \mathbf{A}_1^k to \mathbf{A}_4^k , where k is the index of the image. Each point light source coordinate $\mathbf{L}^k(m, n)$ can be acquired by a linear combination of the four-corner point source coordinates:

$$\begin{aligned} \mathbf{L}^k(m, n) = & \frac{(M-m)(N-n)}{MN} \mathbf{A}_1^k + \frac{(M-m)n}{MN} \mathbf{A}_2^k \\ & + \frac{m(N-n)}{MN} \mathbf{A}_3^k + \frac{mn}{MN} \mathbf{A}_4^k, \end{aligned} \quad (2)$$

where m and n indicate the row and column index of the point light source in the rectangular area, respectively. As shown in Fig. 1(a), one scene point can receive different lighting directions under the near-surface lighting model. We treat the scene image intensity as a linear combination of contributions

from all point light sources, and then we convert Eq. (1) to the near-surface lighting model as follows:

$$\mathbf{I}_p^k \approx \mathbf{R}_p \cdot e \cdot \sum_{mn}^{MN} \frac{\mathbf{N}_p^T(\mathbf{L}^k(m,n) - \mathbf{X}_p)}{\|\mathbf{L}^k(m,n) - \mathbf{X}_p\|^3}. \quad (3)$$

We derive the following objective function D from Eq. (3) by using the method mentioned in [3]:

$$D = 1 - \frac{1}{P \cdot K} \cdot \sum_p \frac{(\sum_k^4 \mathbf{I}_p^k g(\mathbf{L}^k, \mathbf{X}_p))^2}{\sum_k^4 (\mathbf{I}_p^k g(\mathbf{L}^k, \mathbf{X}_p))^2}, \quad (4)$$

where

$$g(\mathbf{L}^k, \mathbf{X}_p) = \frac{1}{\sum_{mn}^{MN} \frac{\mathbf{N}_p^T(\mathbf{L}^k(m,n) - \mathbf{X}_p)}{\|\mathbf{L}^k(m,n) - \mathbf{X}_p\|^3}}. \quad (5)$$

Then, we add two constraint terms for the surface light source and the final energy function is:

$$\begin{aligned} \arg \min D + \lambda \sum_k^4 \sum_{x,y \in N(z)}^4 & [(\mathbf{A}_x^k - \mathbf{A}_z^k)^T \cdot (\mathbf{A}_y^k - \mathbf{A}_z^k)]^2 \\ & + \varphi \sum_{x,y \in N} \sum_{k,j}^4 (\|\mathbf{A}_x^k - \mathbf{A}_y^k\|^2 - \|\mathbf{A}_x^j - \mathbf{A}_y^j\|^2)^2, \end{aligned} \quad (6)$$

where x, y, z are the index of the four corner point light sources, $N(z)$ indicates the neighbors of the z th corner point light source. D is the data term, the second term encourages the the four corner point light sources to form a rectangle and the third term encourages all the rectangle lighting corresponding different images to have the same size.

2.3. Optimization

For the objective function Eq. (6), the aim is to solve the scene normal \mathbf{N} , reflectance \mathbf{R} , coordinates of corner point light sources \mathbf{A} , and power e of each point light source. Directly solving the energy minimization problem is generally difficult because Eq. (6) is a non-convex model with numerous parameters. The optimization result is seriously affected by the initialization. To address this issue, we divide the optimization problem into the following steps:

1. **Estimating \mathbf{A} of each image.** We use gradient descent method to solve the non-linear subproblem.
2. **Calculate the virtual point lighting power.** Refer to Eq. (1), this subproblem has a linear solution assuming all other variables are given.
3. **Obtaining scene normal and reflectance.** Similar to the second subproblem, scene normal \mathbf{N} and reflectance \mathbf{R} can be calculated by a linear solution.
4. **Iteratively solving the three subproblems.** The details of algorithm setting refer to Algorithm 1, where τ is the iteration number, which we set to 20 in all experiments.

2.4. Lighting Reconstruction

After optimizing the objective function Eq. (6), we obtain all the unknown variables. Then we can reconstruct the scene image $\tilde{\mathbf{I}}$ under a given lighting condition through Eq. (3). An integrated algorithm that includes optimization and reconstruction is shown in Algorithm 1. In our experiments, we use only the calculated lighting conditions to render the scene image, which is easy to evaluate the accuracy of reconstruction. In fact, different from traditional methods with the parallel lighting model or near-point lighting model, the near-surface lighting model reflects both the position and orientation as show in Fig. 2(a), and the proposed method has more general reconstruction ability in theory.

Algorithm 1 Optimization method

Input: Multiple images \mathbf{I} under different lighting conditions, parameters M, N, λ, φ and τ ;

- 1: Initialization: $\mathbf{R}_p \leftarrow [1, 1, 1], \mathbf{N}_p \leftarrow [0, 0, 1]$ for all scene points; $\mathbf{A}_1^k \sim \mathbf{A}_4^k \leftarrow [\frac{h}{2}, \frac{w}{2}, \max(h, w)]$, where h and w are image height and width;
- 2: **while** $i < \tau$ **do**
- 3: Calculate \mathbf{A} by gradient descent method through Eq. (6);
- 4: Calculate e by a linear solution through Eq. (1);
- 5: Calculate \mathbf{N}, \mathbf{R} by a linear solution through Eq. (1);
- 6: **end while**
- 7: Generate $\tilde{\mathbf{I}}$ through Eq. (3);

Output: Reconstruction result $\tilde{\mathbf{I}}$.

3. EXPERIMENTAL RESULTS

3.1. Setup

Dataset. We evaluate the proposed method and compare it with previous methods on 6 real scene datasets. These data are from the monitoring of ancient murals in Dunhuang Mogao Grottos. While these ancient cultural relics are seriously protected, they still suffer many types of deteriorations, such as blistering and flaking, as a result, their status are constantly changing in a low speed. To detect reliable minute changes, lighting consistency and recurrence are an important step. On the other side, the surfaces of ancient murals are full of complex structures that make them suitable for evaluating the effect of image reconstruction. For each image scene, we collected 13 images under 1 front lighting and 12 directional side lightings. The directions of side lightings are random in our experiment, and the front lighting is roughly at the front of the scene. We use a handheld LED surface light as light source. The surface light consists of many LED point lattices and is approximately 0.3 ~ 2 meters away from the scene. The images are captured using a Canon 5D Mark III camera.

Baselines and Criterion. To compare the reconstruction accuracy with the proposed novel surface lighting model, we

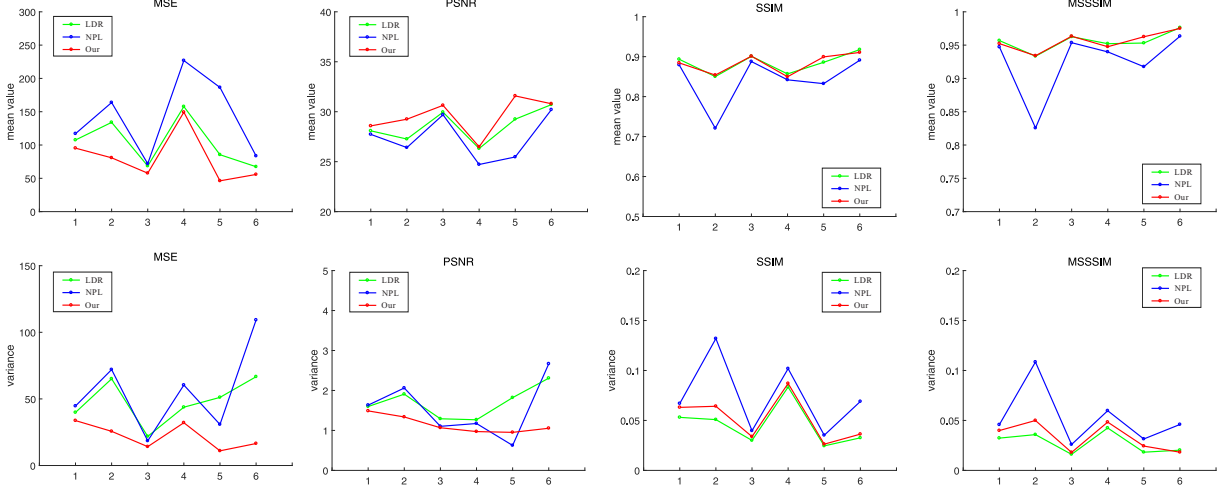


Fig. 3. Mean value and variance of MSE, PSNR, SSIM, MS-SSIM [25] on 6 datasets.

Table 1. Comparison of mean MSE of relighting results under new illuminations of our approach and competitor methods: LDR [8] and near-point Light (NPL) [3].

Method	1	2	3	4	5	6
LDR	107.552	134.000	68.552	157.721	85.438	67.409
NPL	117.074	163.780	71.905	226.821	186.432	83.575
Ours	95.304	80.811	57.732	149.309	46.244	55.810

Table 2. Comparison of mean PSNR of relighting results under new illuminations of our approach and competitor methods: LDR [8] and near-point Light (NPL) [3].

Method	1	2	3	4	5	6
LDR	28.087	27.266	29.955	26.316	29.253	30.709
NPL	27.732	26.410	29.694	24.718	25.471	30.202
Ours	28.580	29.250	30.637	26.487	31.582	30.798

use two state-of-the-art methods as our baselines. One is the Lambertian diffuse reflectance (LDR) method [8] proposed by Favaor et al., which introduces LDR maxima to solve the uncalibrated photometric stereo and only considers parallel lighting in its model. The other is the near-point lighting model (NPL) [3], which considers lighting distance and has been described previously. We use MSE, PSNR, SSIM and MS-SSIM [25] to measure the similarity between the original and reconstructed images. And these four criteria are widely used in image quality comparison.

Implementation Details. All codes are implemented using Matlab. We use Gaussian-Newton iteration to optimize the results. The parameters in each dataset are the same. For λ and φ , we use $height \times width \times 10^{-12}$ in our experiment. For rectangle lighting size, we use $M = 8$ and $N = 8$, and the optimizing iterations are always 20.

3.2. Quantitative comparison

Using 13 images in each dataset as input, we solve the scene normal, reflectance, and lighting positions by the proposed method, and then the scene image under each given lighting condition is recovered. We then compare image reconstruc-

Table 3. Comparison of mean SSIM of relighting results under new illuminations of our approach and competitor methods: LDR [8] and near-point Light (NPL) [3].

Method	1	2	3	4	5	6
LDR	0.8934	0.8501	0.9008	0.8568	0.8858	0.9176
NPL	0.8794	0.7209	0.8877	0.8420	0.8324	0.8910
Ours	0.8844	0.8539	0.9012	0.8497	0.8994	0.9105

Table 4. Comparison of mean MS-SSIM of relighting results under new illuminations of our approach and competitor methods: LDR [8] and near-point Light (NPL) [3].

Method	1	2	3	4	5	6
LDR	0.9568	0.9333	0.9626	0.9521	0.9531	0.9762
NPL	0.9472	0.8256	0.9536	0.9398	0.9176	0.9634
Ours	0.9522	0.9340	0.9633	0.9476	0.9625	0.9750

tion accuracy with baselines under all 13 lighting conditions. Fig. 3 illustrates the detailed mean value and variance of 4 criterions with 13 image reconstruction results for each scene, and Table 1 ~ 4 show detailed numerical results. Both the figures and the tables show that the proposed method always has the superior performance on both mean value and variation, the MSE and PSNR values are always best in comparison, with 75% promotion of MSE at most. And 3 out of 6 are best on SSIM and MS-SSIM criteria, the other 3 gain the second highest score and are quite close to the best one, with at most 1.01% SSIM score and 0.48% MS-SSIM score lower than the best.

Fig. 4 presents the visual results of the baseline and the proposed method, labeled with MSE value in each reconstruction image. Each two rows are corresponding to a scene dataset, we choose two lighting results from each dataset. The reconstruction image and its difference image with original are displayed. To make a clear show effect, the difference images are all multiplied by 5. Through visual comparison, we see that the LDR method cannot correctly recover the image color information mainly because of its computational error of reflectance, And near-point lighting model shows much more errors in difference images. By contrast, our proposed

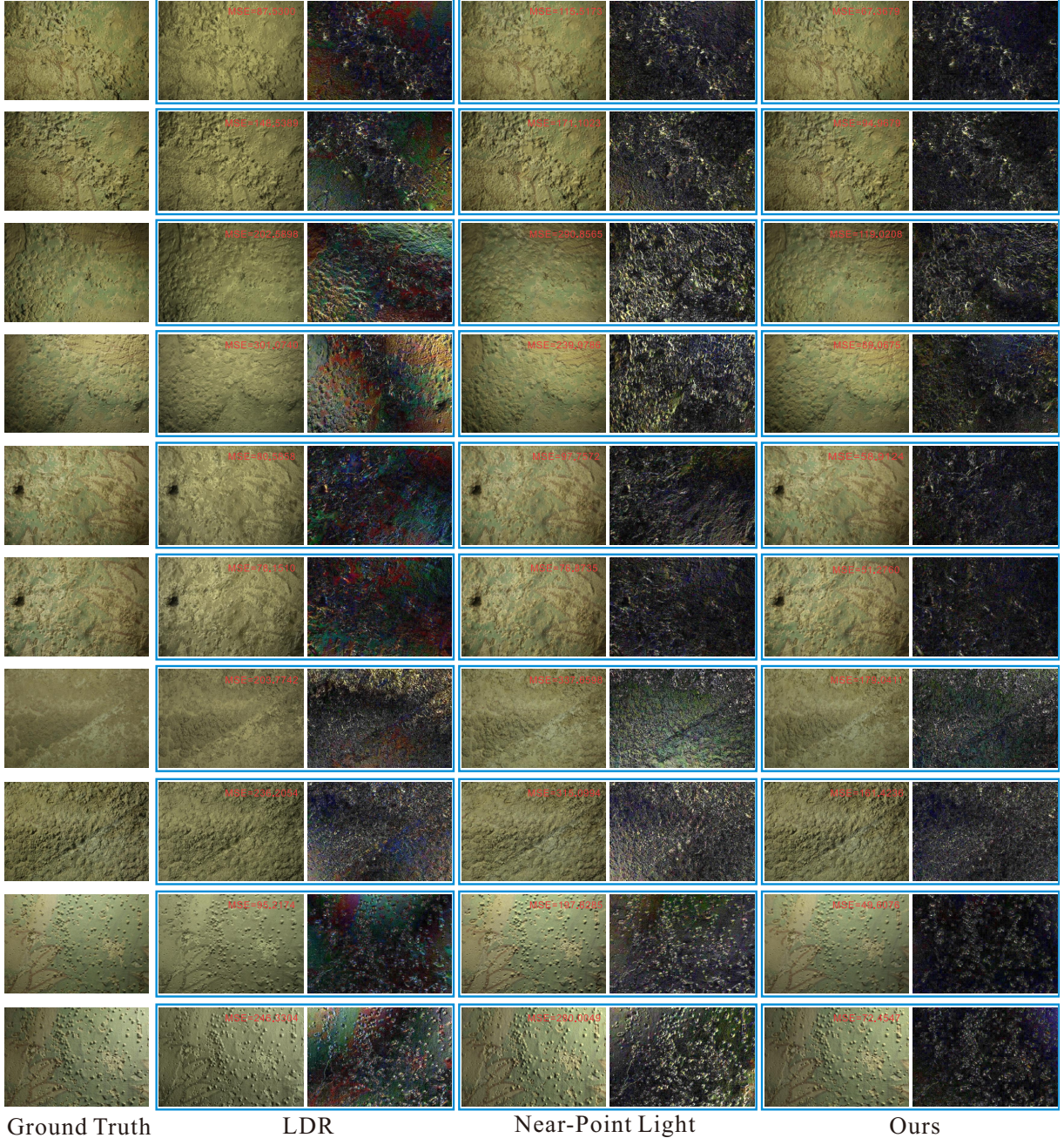


Fig. 4. Comparative results of relighting under new illuminations of our approach and competitor methods.

method exhibits superior results for both visual perception and MSE value.

4. CONCLUSION

In this paper, we have proposed a novel near-surface lighting model for lighting estimation and new lighting reconstruction. In contrast to classical methods, our approach considers a much more realistic and general lighting model, i.e., near-surface light model, which has been formulated as a regular

grid of near-point lighting sources. We present an effective joint optimization solution to decompose such new lighting model together with the scene normal and reflectance. Besides, our approach is an calibration-free model and does not need any prior knowledge about the light source. Extensive experiments validate the effectiveness and superiority of the proposed approach over state-of-the-arts based on parallel lighting and near-point lighting models. In the future, we intend to improve our approach to make surface lighting size to be self-determined and make it more general to fit other lighting structures.

5. REFERENCES

- [1] M. Tom, G. Dan, and W. Hans, “Polynomial texture maps,” in *ICME*, ACM, 2001.
- [2] S.Y. Elhabian, R. Ham, and A.A. Farag, “Towards accurate and efficient representation of image irradiance of convex-lambertian objects under unknown near lighting,” in *ICCV*, 2011.
- [3] X. Huang, M. Walton, G. Bearman, and O. Cossairt, “Near light correction for image relighting and 3d shape recovery,” in *Digital Heritage*, 2015.
- [4] R.J. Woodham, “Photometric method for determining surface orientation from multiple images,” *Optical engineering*, vol. 19, no. 1, 1980.
- [5] W.M. Silver, “Determining shape and reflectance using multiple images,” in *MIT*, 1980.
- [6] J. Ahmad, J. Sun, L. Smith, and M. Smith, “An improved photometric stereo through distance estimation and light vector optimization from diffused maxima region,” *Pattern Recognition Letters*, vol. 50, pp. 15–22, 2014.
- [7] I. Sato, T. Okabe, Q. Yu, and Y. Sato, “Shape reconstruction based on similarity in radiance changes under varying illumination,” in *ICCV*, 2007.
- [8] P. Favaro and T. Papadimitri, “A closed-form solution to uncalibrated photometric stereo via diffuse maxima,” in *CVPR*, 2012.
- [9] F. Lu, Y. Matsushita, I. Sato, T. Okabe, and Y. Sato, “Uncalibrated photometric stereo for unknown isotropic reflectances,” in *CVPR*, 2013.
- [10] F. Lu, I. Sato, and Y. Sato, “Uncalibrated photometric stereo based on elevation angle recovery from brdf symmetry of isotropic materials,” in *CVPR*, 2015.
- [11] N. G. Alldrin, T. Zickler, and D. J. Kriegman, “Photometric stereo with non-parametric and spatially-varying reflectance,” in *CVPR*, 2008.
- [12] N. G. Alldrin, S. P. Mallick, and D. J. Kriegman, “Resolving the generalized bas-relief ambiguity by entropy minimization,” in *CVPR*, 2007.
- [13] B. Shi, Tan. P., and Y. Matsushita, “A biquadratic reflectance model for radiometric image analysis,” in *CVPR*, 2012.
- [14] B. Shi, P. Tan, Y. Matsushita, and K. Ikeuchi, “Elevation angle from reflectance monotonicity: Photometric stereo for general isotropic reflectances,” in *ECCV*, 2012.
- [15] S. Ikehata and K. Aizawa, “Photometric stereo using constrained bivariate regression for general isotropic surfaces,” in *CVPR*, 2014.
- [16] C. Inoshita, Y. Mukaigawa, and Y. Matsushita, “Surface normal deconvolution: Photometric stereo for optically thick translucent objects,” in *ECCV*, 2014.
- [17] Z. Hui and A. C. Sankaranarayanan, “A dictionary-based approach for estimating shape and spatially-varying reflectance,” in *ECCV*, 2014.
- [18] F. Sakaue and J. Sato, “A new approach of photometric stereo from linear image representation under close lighting,” in *ICCV*, 2011.
- [19] A. Wetzler, R. Kimmel, A. M. Bruckstein, and R. Mecca, “Close-range photometric stereo with point light sources,” in *International Conference on 3D Vision*, 2014.
- [20] W. Xie, C. Dai, and C. C. Wang, “Photometric stereo with near point lighting: A solution by mesh deformation,” in *CVPR*, 2015.
- [21] E. Prados and O. Faugeras, “Unifying approaches and removing unrealistic assumptions in shape from shading: Mathematics can help,” in *ECCV*, 2004.
- [22] T. Okabe and Y. Sato, “Effects of image segmentation for approximating object appearance under near lighting,” in *ACCV*, 2006.
- [23] T. Papadimitri and P. Favaro, “Uncalibrated near-light photometric stereo,” in *BMVC*, 2014.
- [24] D. Frolova, D. Simakov, and R. Basri, “Accuracy of spherical harmonic approximations for images of lambertian objects under far and near lighting,” in *ECCV*, 2004.
- [25] Zhou Wang, Eero P Simoncelli, and Alan C Bovik, “Multiscale structural similarity for image quality assessment,” in *IEEE Asilomar Conference on Signals, Systems and Computers*, 2003.